Periodico di Mineralogia (20134, 83, 1, 1-18 DOI: 10.2451/2014PM0001

PERIODICO di MINERALOGIA
established in 1930

An International Journal of
MINERALOGY, CRYSTALLOGRAPHY, GEOCHEMISTRY, ORE DEPOSITS, PETROLOGY, VOLCANOLOGY
and applied topics on *Environment*, *Archaeometry* and *Cultural Heritage*

Mercury-arsenic sulfosalts from the Apuan Alps (Tuscany, Italy). III. Aktashite, $Cu_6Hg_3As_4S_{12}$, and laffittite, $AgHgAsS_3$, from the Monte Arsiccio mine: occurrence and crystal structure

Cristian Biagioni[1,*], Elena Bonaccorsi[1], Yves Moëlo[2] and Paolo Orlandi[1]

[1]Dipartimento di Scienze della Terra, Università di Pisa, Via S. Maria 53, I-56126 Pisa, Italy
[2]Institut des Matériaux Jean Rouxel, UMR 6502, CNRS, Université de Nantes, 2 rue de la Houssinière, 44 322 Nantes Cedex 3, France
*Corresponding author: *biagioni@dst.unipi.it*

Abstract

Aktashite, ideally $Cu_6Hg_3As_4S_{12}$, and laffittite, $AgHgAsS_3$, were identified on specimens from the Monte Arsiccio mine, Apuan Alps, Tuscany, Italy, on the basis of X-ray diffraction and chemical data. Aktashite and laffittite occur as anhedral grains, up to 0.5 mm in size, in the pyrite-rich dolostone and in the baryte + pyrite microcrystalline ore bodies from the Sant'Olga level. Associated minerals are baryte, boscardinite, cymrite, protochabournéite, pyrite, realgar, Hg-rich sphalerite, stibnite, and some still unidentified phases. Electron-microprobe data of aktashite point to the following composition (in wt%): Cu 22.53(28), Ag 0.75(16), Fe 0.20(12), Hg 33.28(41), Zn 0.43(2), Cd 0.07(6), As 14.33(22), Sb 4.71(30), S 22.93(9), Se 0.15(15), total 99.39(25). The structural formula, based on 13 cations per formula unit, is $(Cu_{6.00}Fe_{0.06})_{\Sigma 6.06}(Hg_{2.81}Ag_{0.12}Zn_{0.11}Cd_{0.01})_{\Sigma 3.05}(As_{3.24}Sb_{0.66})_{\Sigma 3.90}(S_{12.10}Se_{0.03})_{\Sigma 12.13}$. Laffittite was only qualitatively analyzed, showing Hg, Ag, As, S, and minor Sb as the only elements with $Z > 9$. The crystal structures of aktashite and laffittite were refined to $R_1 = 0.0264$ and 0.0285, respectively. Aktashite is trigonal, $R3$, with unit-cell parameters a 13.7752(14), c 9.3785(10) Å, V 1541.2(3) Å^3; laffittite is monoclinic, space group Cc, with unit-cell parameters a 6.6671(2), b 11.3334(3), c 7.7572(2) Å, β 115.258(2)°, V 530.10(3) Å^3. Their crystal structures are three-dimensional frameworks formed by Cu-, Ag-, and Hg-centred tetrahedra, connected through corner-sharing with isolated AsS_3 trigonal pyramids. Both phases show Hg in four-fold coordination. The dissymmetry of tetrahedral Hg site in laffittite (2+2, i.e. two shorter and two

longer bonds) relatively to aktashite (regular tetrahedral) is correlated to a similar dissymmetry of Ag *versus* Cu coordinations. Aktashite and laffittite increase the list of rare Hg sulfides and sulfosalts identified in the baryte-pyrite-iron oxides deposits from Apuan Alps.

Key words: aktashite; laffittite; sulfosalt; mercury; arsenic; crystal structure.

Introduction

The Monte Arsiccio mine (latitude 43°58' N; longitude 10°17'E) exploited a small baryte-pyrite-iron oxides deposit in the Apuan Alps (Costagliola et al., 1990). Its complex mineralogy is currently under study and two new thallium-lead sulfosalts were recently described, boscardinite and protochabournéite (Orlandi et al., 2012; Orlandi et al., 2013). Recently, Biagioni et al. (2013b) described an exceptional Tl-Hg-As-Sb-(Ag,Cu)-Pb mineralization at the Sant'Olga level. Among Hg sulfosalts observed here, routhierite and the new mineral arsiccioite have been described (Biagioni et al., 2013a; Biagioni et al., 2014). The present study deals with two other very rare Hg sulfosalts occurring in the same mineral assemblage, aktashite, $Cu_6Hg_3As_4S_{12}$, and laffittite, $AgHgAsS_3$.

Vasil'ev (1968) described a new mercury-arsenic sulfosalt from the Aktash Hg deposit, Gorny Altai, Russia, provisionally naming it aktashite. The phase was associated with quartz, pyrite, calcite, sphalerite, stibnite, chalcostibite, mercurian tetrahedrite, tennantite, luzonite, enargite, chalcopyrite, cinnabar, dickite, and orpiment. Gruzdev et al. (1972) described a new occurrence of aktashite from the Galkhaya deposit, reporting new chemical and crystallographic data, and confirmed that this phase is a new and valid mineral species. However, aktashite was never officially approved by the IMA Commission on New Minerals and Mineral Names (CNMNM). Other occurrences of aktashite are known (e.g., Chauvai Hg deposit – Spiridonov et al., 1981; Hemlo, Ontario, Canada – Powell and Pattison, 1997; Escarlati Sb-Hg deposit, León, Spain – Martín-Izard et al., 2009). The crystal structure of aktashite was solved by Kaplunnik et al. (1980) and recently refined by Vasil'ev et al. (2010). Aktashite belongs to the nowackiite isotypic series, together with nowackiite, $Cu_6Zn_3As_4S_{12}$, and gruzdevite, $Cu_6Hg_3Sb_4S_{12}$ (Moëlo et al., 2008).

With respect to aktashite, laffittite is definitely rarer, being described only from three localities world-wide. It was first found in the thallium mineralization of Jas Roux, Hautes-Alpes, France (Johan et al., 1974), in association with routhierite, realgar, and thallium-antimony sulfosalts. In addition to the type locality, laffittite has been found in two other localities: Getchell mine, Nevada, USA (Nakai and Appleman, 1983), and Chauvai, Kyrgyzstan (Pervukhina et al., 2010a). Its crystal structure was solved by Nakai & Appleman (1983).

The new findings of aktashite and laffittite from the Monte Arsiccio mine allowed us to collect new structural and chemical data,

reporting additional information on these two mercury-arsenic sulfosalts.

Occurrence and Mineral description

Occurrence and physical properties

The geological setting of the Monte Arsiccio mine has been described in previous papers (Costagliola et al., 1990; Orlandi et al., 2012). Ore bodies are embedded in the phyllitic "Scisti di Fornovolasco" Formation and at the contact between this formation and the overlying Grezzoni Formation of Upper Triassic age. In the Sant'Olga level, in proximity to the old inclined shaft connecting Sant'Olga with the upper Sant'Anna level, a dolostone lens occurs at the contact with the footwall schists and the baryte + pyrite ore. The ore is represented by a conformable lens formed by microcrystalline baryte + pyrite, associated with minor amounts of Hg-Tl-Pb-Ag-Sb-As sulfosalts, sphalerite, stibnite, and realgar. These phases show textures interpreted by Biagioni et al. (2013b) as the result of the crystallization from a sulfosalt melt during the Alpine metamorphism of the Monte Arsiccio ore deposit. The lens of dolostone is characterized by vein systems, often containing rare mineral species (e.g., mannardite – Biagioni

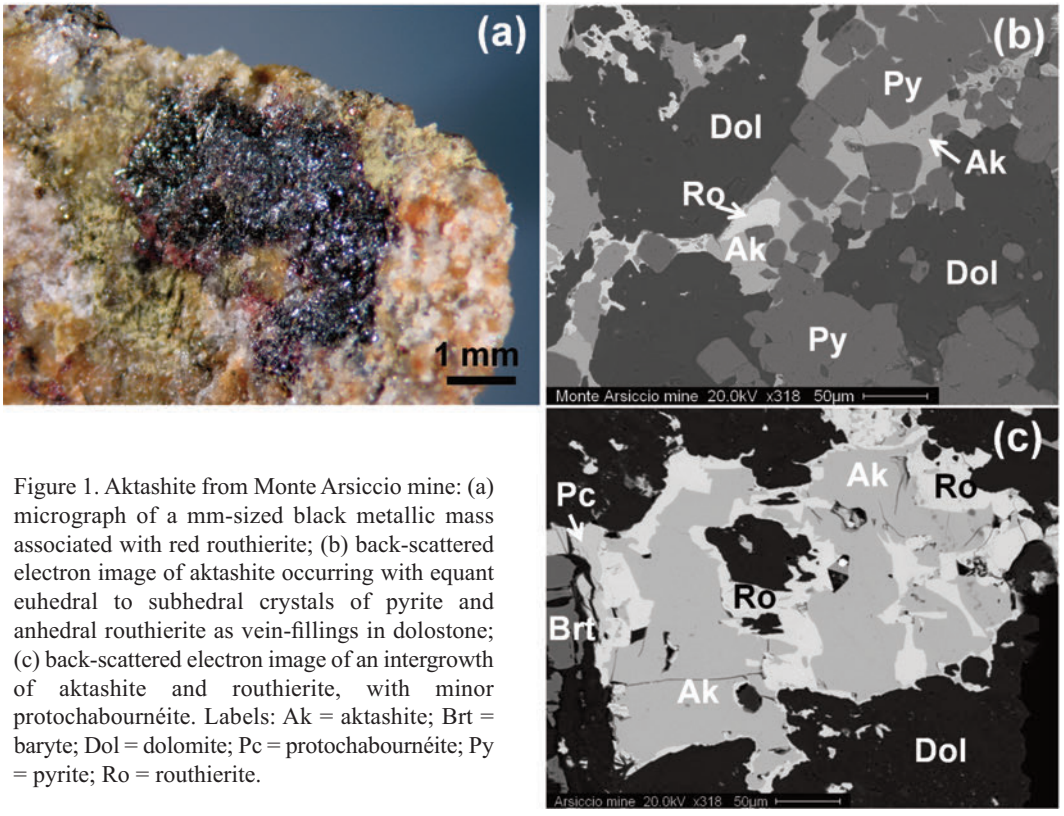

Figure 1. Aktashite from Monte Arsiccio mine: (a) micrograph of a mm-sized black metallic mass associated with red routhierite; (b) back-scattered electron image of aktashite occurring with equant euhedral to subhedral crystals of pyrite and anhedral routhierite as vein-fillings in dolostone; (c) back-scattered electron image of an intergrowth of aktashite and routhierite, with minor protochabournéite. Labels: Ak = aktashite; Brt = baryte; Dol = dolomite; Pc = protochabournéite; Py = pyrite; Ro = routhierite.

et al., 2009), along with thallium sulfosalts. These minerals have been found in two different occurrences within the dolostone: i) in quartz + baryte + dolomite veins, and ii) as sulfide veins. This latter kind of occurrence is particularly well-developed near the contact between the footwall schists and the dolostone lens, which becomes enriched in pyrite and other sulfides. Aktashite was identified in this latter occurrence, along the inclined shaft connecting the Sant'Olga level with the lower ones. Laffittite was also identified once in the sulfide veins, but it also occurs in the baryte + pyrite microcrystalline conformable lens embedded in the schists.

In hand-specimens, aktashite occurs as blackish compact masses, up to 5 mm in size, always associated with routhierite. It has a sub-metallic luster and an irregular to conchoidal fracture. Scanning electron microscopy revealed the usual intergrowth of aktashite and routhierite; rarely, aktashite forms veinlets surrounding euhedral to subhedral equant pyrite crystals (Figure 1). In addition to routhierite, aktashite is also associated with protochabournéite.

Laffittite occurs as sub-millimeter sized grains, red in color, transparent in tiny fragments and with an adamantine luster. In the sulfide veins hosted in the dolostone, laffittite was observed in only one polished section, as rounded anhedral grains, up to 50 μm in size, included in a still unidentified Ag-Sb-As sulfosalt (on the basis of a semi-quantitative EDS analysis this phase could tentatively be identified as an As-rich variety of miargyrite). Boscardinite, protochabournéite, and routhierite also occur in the same polished section. Laffittite was observed more frequently in the baryte + pyrite ore body, as a component of polyphasic grains in the interstices of microcrystalline baryte. In the specimens studied, laffittite is associated with protochabournéite and realgar, in grains up to 100 μm in size (Figure 2).

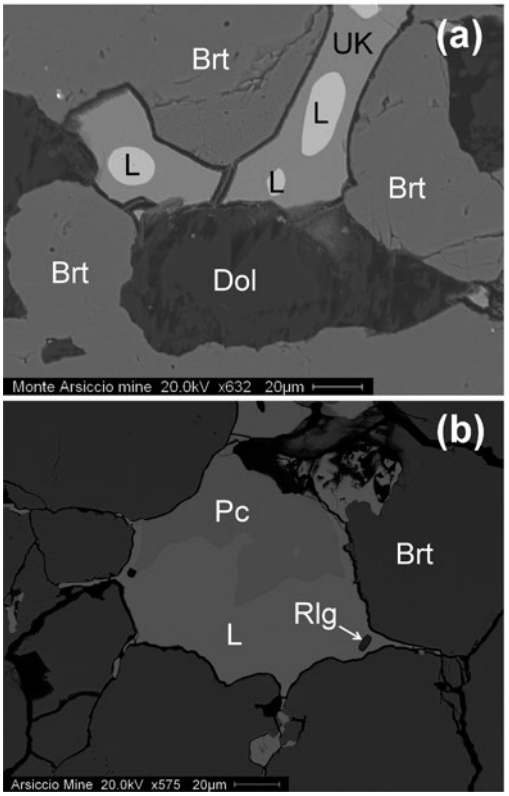

Figure 2. Back-scattered electron images of laffittite from Monte Arsiccio mine: (a) anhedral grains of laffittite included in an unidentified Ag-Sb-As sulfosalt from the pyrite-rich dolostone; (b) anhedral grain closely associated with protochabournéite and realgar, in the microcrystalline baryte. Same labels as in Fig. 1; in addition L = laffittite; Rlg = realgar; UK = unknown Ag-Sb-As sulfosalt.

Chemical data

Preliminary qualitative chemical analyses were performed using a Phillips XL30 scanning electron microscope equipped with an EDAX DX4 system. The only elements with $Z > 9$ detected in aktashite were Cu, Hg, As, S, and minor Sb; Hg, Ag, As, S, and a very limited amount of Sb for laffittite. Quantitative data were collected for aktashite only; in fact, owing to the small size of the only available grain of laffittite, it was not possible to prepare it for electron-microprobe analysis.

Quantitative electron-microprobe data were collected using a CAMECA SX100 electron-microprobe. Operating conditions were: accelerating voltage 20 kV, beam current 20 nA, beam size 2 μm. Standards used were (element, emission line, counting time): HgS (Hg *Mα*, 20 s), $TlAsS_2$ (Tl *Mα*, 20 s), AsGa (As *Lα*, 40 s), Sb_2S_3 (Sb *Lα*, 30 s), pyrite (S *Kα*, 50 s; Fe *Kα*, 20 s), Ag (Ag *Lα*, 30 s), Cu (Cu *Kα*, 30 s), ZnS (Zn *Kα*, 20 s), Cd (Cd *Lα*, 10 s), and Se (Se *Lα*, 40 s). Analytical data are given in Table 1.

The chemical formula, based on 13 cations per formula unit, corresponds to $(Cu_{6.00(5)}Fe_{0.06(4)})_{\Sigma 6.06}(Hg_{2.81(4)}Ag_{0.12(3)}Zn_{0.11(1)}Cd_{0.01(1)})_{\Sigma 3.05}(As_{3.24(6)}Sb_{0.66(4)})_{\Sigma 3.90}S_{12.10(5)}Se_{0.03(3)}$. Iron was assumed as trivalent, like in copper sulphides related to the sphalerite archetype. Aktashite shows only minor deviations from the ideal stoichiometry. Vasil'ev et al. (2010) reported chemical analyses from different Russian occurrences. The Sb content of aktashite from Monte Arsiccio is higher than those of the majority of aktashite occurrences; only aktashite from Makratela has a similar Sb content (4.80 wt%). This is in agreement with the As-Sb substitution in the series aktashite-gruzdevite ($Cu_6Hg_3Sb_4S_{12}$).

Table 1. Microprobe analyses of aktashite (n = 3): chemical composition as wt% and number of atoms on the basis of ΣMe = 13 apfu.

Element	wt%	apfu
Cu	22.53(28)	6.00(5)
Ag	0.75(16)	0.12(3)
Fe	0.20(12)	0.06(4)
Hg	33.28(41)	2.81(4)
Zn	0.43(2)	0.11(1)
Cd	0.07(6)	0.01(1)
As	14.33(22)	3.24(6)
Sb	4.71(30)	0.66(4)
S	22.93(9)	12.10(5)
Se	0.15(15)	0.03(3)
Total	99.39(25)	Ev = - 1.8(1)

Ev: relative error (%) on the valence equilibrium

Crystallography

Aktashite was preliminarily identified through X-ray powder diffraction, using a 114.6 mm diameter Gandolfi camera, with Ni-filtered Cu *K*α radiation. Laffittite was identified using single-crystal X-ray diffraction.

Intensity data were collected using a Bruker Smart Breeze diffractometer, with air-cooled CCD detector and graphite-monochromatized Mo *K*α radiation; the detector-to-crystal working distance was 50 mm. Frames were collected using φ and ω scan modes, in 0.5° slices. Intensity data were integrated and corrected for Lorentz, polarization, background effects, and absorption using the package of software APEX2 (Bruker AXS Inc., 2004). The crystal structures

of aktashite and laffittite were refined using SHELX-97 (Sheldrick, 2008). Scattering curves for neutral atoms were taken from the *International Tables for X-ray Crystallography* (Wilson, 1992). Details of the data collection and crystal structure refinement are reported in Table 2. Table 3 reports atomic coordinates, site occupancies, and equivalent isotropic displacement parameters, whereas Table 4 gives anisotropic displacement parameters for both species.

Aktashite. Two datasets of 637 frames were collected in ω scan mode, with exposure time of 20 seconds and scan width 0.5° per frame. The refined unit-cell parameters are *a* 13.7752(14), *c*

Table 2. Crystal data and summary of parameters describing data collection and refinement for aktashite and laffittite.

	Aktashite	*Laffittite*
Crystal data		
X-ray formula	$(Cu_{5.16}Hg_{0.84})(Hg_{2.01}Cu_{0.99})(As_{3.42}Sb_{0.58})S_{12}$	$AgHg(As_{0.92}Sb_{0.08})S_3$
Crystal size (mm^3)	0.11 x 0.08 x 0.05	0.10 x 0.08 x 0.04
Cell setting, space group	Trigonal, *R*3	Monoclinic, *Cc*
Unit cell dimensions		
a (Å)	13.7752(14)	6.6671(2)
b (Å)	13.7752(14)	11.3334(3)
c (Å)	9.3785(10)	7.7572(2)
β (°)		115.258(2)
V ($Å^3$)	1541.2(3)	530.10(3) *Z* 3 4
Data collection and refinement		
Radiation type, (λ)	Mo *K*α (0.71073 Å)	
Temperature	room	
Maximum observed 2θ(°)	71.33	65.19
Measured reflections	4122	2760
Unique reflections	2280	1466
Reflections $F_o > 4\sigma F_o$	2024	1374
R_{int}	0.0206	0.0234
*R*σ	0.0644	0.0586
Range of *h*, *k*, *l*	$-18 \le h \le 19$	$-9 \le h \le 10$
	$-22 \le k \le 17$	$-14 \le k \le 17$
	$-15 \le l \le 14$	$-11 \le l \le 11$
R_1 [$F_o > 4\sigma F_o$]	0.0264	0.0285
R_1 (all data)	0.0340	0.0315
wR_2 (on F_o^2)	0.0613	0.0619
Goof	0.753	0.969
Number of l.s. parameters	82	57
$\Delta\rho_{max}$ and $\Delta\rho_{min}$	1.51 (at 0.59 Å from Hg)	1.03 (at 1.57 Å from Hg)
	- 0.96 (at 1.18 Å from Cu2)	-2.28 (at 0.68 Å from Hg)

Table 3. Atomic coordinates, site occupancies, and equivalent displacement parameters (Å^2) for aktashite and laffittite.

Aktashite

Site	occupancy	*x*	*y*	*z*	U_{eq}
Hg	$Hg_{0.67(1)}Cu_{0.33(1)}$	0.10318(6)	0.36056(5)	0.69574(3)	0.0292(1)
Cu1	$Cu_{0.98(1)}Hg_{0.02(1)}$	0.05301(10)	0.15870(9)	0.38095(7)	0.0266(3)
Cu2	$Cu_{0.74(1)}Hg_{0.26(1)}$	0.22330(6)	0.29549(5)	0.04058(6)	0.0284(2)
As1	$As_{0.82(1)}Sb_{0.18(1)}$	0.27857(7)	½	0.36982(8)	0.0163(2)
As2	$As_{0.89(1)}Sb_{0.11(1)}$	1/3	2/3	0.68285(9)	0.0145(3)
S1	$S_{1.00}$	0.10750(11)	0.34916(11)	0.43256(16)	0.0210(3)
S2	$S_{1.00}$	0.27063(12)	0.47499(12)	0.12902(14)	0.0191(3)
S3	$S_{1.00}$	0.17052(12)	0.54872(12)	0.80019(13)	0.0203(3)
S4	$S_{1.00}$	0.23001(12)	0.29302(12)	0.78604(17)	0.0226(3)

Laffittite

Site	occupancy	*x*	*y*	*z*	U_{eq}
Hg	$Hg_{1.00}$	0.02980(8)	0.31691(3)	0.78997(7)	0.0280(1)
Ag	$Ag_{1.00}$	-0.00123(10)	0.02115(6)	0.25057(8)	0.0305(2)
As	$As_{0.92(1)}Sb_{0.08(1)}$	0.02042(16)	0.35172(6)	0.28688(14)	0.0141(2)
S1	$S_{1.00}$	0.4316(3)	0.0090(2)	0.4225(2)	0.0153(3)
S2	$S_{1.00}$	0.4698(3)	0.2855(2)	0.9857(2)	0.0150(3)
S3	$S_{1.00}$	0.3961(3)	0.3710(2)	0.4389(2)	0.0162(3)

9.3785(10) Å, *V* 1541.2(3) Å^3, space group *R*3. The atomic coordinates given by Vasil'ev et al. (2010) were used as a starting model. After some cycles of isotropic refinement, the *R* value converged to 10.8 %, confirming the validity of the structural model. The occupancy of the five independent cation sites were refined using the following scattering factor curves: Hg, Cu1, and Cu2 sites: Hg *vs* Cu; As1 and As2 sites: As *vs* Sb. Cu1 is a quite pure Cu site, whereas an electron density lower than the expected one was found at the Hg site and an higher density was observed at the Cu2 site. As these two latter sites can be related by a rotation of 60° around the triad axis, the presence of twinning was tested through the matrix [0 -1 0| 1 1 0| 0 0 1], as a possible explanation of these two electron-density shifts. The result of the refinement indicated that this twin law was not operating in the studied crystals. The refined cation site scattering, for *Z* = 3, is 548.8 electrons per formula unit (epfu), in agreement with the value calculated from electron-microprobe data, that is 550.4 epfu. After the introduction of the anisotropic displacement parameters, the refinement converged to R_1 = 2.64 % for 2024 observed reflections.

Laffittite. Five datasets of 932 frames were collected in ω scan mode, with exposure time of

Table 4. Anisotropic displacement parameters (Å^2) for aktashite and laffittite.

Aktashite

Site	U^{11}	U^{22}	U^{33}	U^{23}	U^{13}	U^{12}
Hg	0.0263(2)	0.0242(2)	0.0317(2)	-0.0013(1)	0.0019(1)	0.0084(1)
Cu1	0.0246(5)	0.0351(6)	0.0219(4)	-0.0009(3)	-0.0005(3)	0.0163(5)
Cu2	0.0281(4)	0.0216(3)	0.0317(3)	-0.0024(2)	0.0005(2)	0.0095(3)
As1	0.0170(4)	0.0129(3)	0.0192(2)	-0.0008(2)	0.0013(2)	0.0077(3)
As2	0.0156(3)	0.0156(3)	0.0122(5)	0	0	0.0078(2)
S1	0.0193(7)	0.0148(6)	0.0255(6)	0.0006(4)	0.0053(5)	0.0061(5)
S2	0.0178(6)	0.0228(7)	0.0182(6)	0.0050(4)	0.0025(4)	0.0111(5)
S3	0.0127(6)	0.0263(7)	0.0152(5)	0.0022(4)	0.0002(4)	0.0048(5)
S4	0.0290(8)	0.0197(7)	0.0220(6)	-0.0035(5)	-0.0025(5)	0.0142(6)

Laffittite

Site	U^{11}	U^{22}	U^{33}	U^{23}	U^{13}	U^{12}
Hg	0.0327(2)	0.0238(2)	0.0323(2)	-0.0076(2)	0.0185(1)	-0.0012(2)
Ag	0.0291(4)	0.0325(4)	0.0316(5)	0.0123(3)	0.0146(4)	0.0032(3)
As	0.0161(3)	0.0124(4)	0.0156(3)	-0.0012(4)	0.0084(2)	-0.0022(4)
S1	0.0192(7)	0.0129(8)	0.0179(7)	-0.0006(6)	0.0118(6)	-0.0003(6)
S2	0.0162(6)	0.0127(7)	0.0163(6)	0.0013(6)	0.0071(5)	0.0019(6)
S3	0.0166(7)	0.0149(8)	0.0203(7)	-0.0005(6)	0.0110(6)	0.0005(6)

30 seconds per frame. The refined unit-cell parameters are *a* 6.6671(2), *b* 11.3334(3), *c* 7.7572(2) Å, β 115.258(2)°, *V* 530.10(3) Å^3, space group *Cc*. The statistical tests on the distribution of $|E|$ values ($|E^2-1| = 0.867$) agrees with the absence of an inversion center. As starting point, the atomic coordinates given by Pervukhina et al. (2010a) were used, transformed from the space group *Aa* into the space group *Cc*. After ten cycles of isotropic refinement, the *R* value converged to 7.6 %, thus confirming the validity of the structural model. The occupancies of the three independent cation sites were refined using the scattering factor curves of Hg, Ag, and As *vs* Sb, for Hg, Ag, and As sites, respectively. Refining the site occupancies and introducing the anisotropic displacement parameters led the refinement to converge to $R_1 = 2.85\%$ for 1374 observed reflections.

Crystal structure description

In agreement with the crystal structure studies of Kaplunnik et al. (1980) (refined by Vasil'ev et al., 2010), and Nakai and Appleman (1983), respectively, aktashite and laffittite display a 3D-framework of Cu-, Ag-, and Hg-centered tetrahedra, connected through corner-sharing to isolated AsS_3 trigonal pyramids, giving rise to different structural arrangements. Table 5 gives selected bond distances for aktashite and laffittite.

Table 5. Selected bond distances (in Å) in aktashite and laffittite.

Aktashite

Hg	– S1	2.470(2)	Cu1	– S2	2.276(2)	Cu2	– S2	2.370(2)
	– S1	2.476(2)		– S2	2.302(2)		– S3	2.377(2)
	– S3	2.477(2)		– S3	2.325(2)		– S4	2.382(2)
	– S4	2.502(2)		– S1	2.390(2)		– S4	2.390(2)
	average	2.481		average	2.323		average	2.380
As1	– S2	2.279(1)	As2	– S3	2.288(2)^{x3}			
	– S1	2.307(2)						
	– S4	2.327(2)						
	average	2.304						

Laffittite

Hg	– S1	2.440(2)	Ag	– S1	2.520(2)	As1	– S1	2.273(2)
	– S2	2.504(2)		– S2	2.529(2)		– S3	2.279(2)
	– S2	2.690(2)		– S2	2.616(2)		– S2	2.314(2)
	– S3	2.746(2)		– S3	2.910(2)		average	2.289
	average	2.595		average	2.644			

Crystal structure of aktashite

The crystal structure of aktashite can be described as formed by (0001) layers composed of corner-sharing HgS_4 and CuS_4 tetrahedra, delimiting two triangular cavities (Figure 3). In the larger one (A in Figure 3), three As1

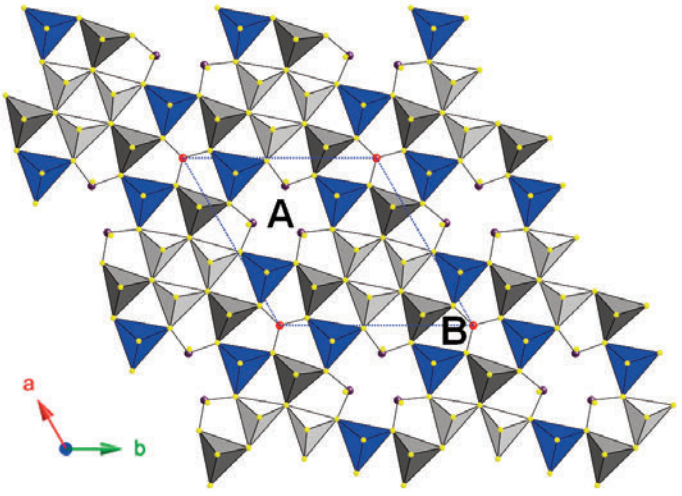

Figure 3. Crystal structure of aktashite as seen down [0001]. Polyhedra: blue = Hg site; dark grey = Cu1 site; light grey = Cu2 site. Circles: violet = As1 site; red = As2 site; yellow = S sites.

Table 6. Site occupancies, refined and calculated site scattering for Hg and Cu sites in aktashite.

Site	*Site occupancy*	*Calculated site scattering*	*Refined site scattering*
Hg	$Hg_{0.65}Cu_{0.31}Ag_{0.04}$	62.9	63.2
Cu1	$Cu_{1.00}$	29.0	30.0
Cu2	$Cu_{0.69}Hg_{0.26}Zn_{0.03}Fe^{3+}{}_{0.02}$	42.2	42.3

Table 7. Bond-valence calculations (according to Brese and O'Keeffe, 1991) for aktashite and laffittite.

Aktashite

Site	*S1*	*S2*	*S3*	*S4*	*Σ cations*	*Theor.*
Hg	0.51 0.50		0.50	0.47	1.98	1.65
Cu1	0.24	0.32 0.30	0.28		1.14	1.00
Cu2		0.43	0.41	0.42 0.40	1.66	1.33
As1	0.99	1.07		0.94	3.00	3.00
As2			0.99x3		2.97	3.00
Σ anions	2.24	2.12	2.18	2.21		
Theor.	2.00	2.00	2.00	2.00		

Laffittite

Site	*S1*	*S2*	*S3*	*Σ cations*	*Theor.*
Hg	0.72	0.61 0.37	0.32	2.02	2.00
Ag	0.28	0.13	0.37 0.36	1.14	1.00
As	1.02	0.91	1.00	2.93	3.00
Σ anions	2.02	2.02	2.05		
Theor.	2.00	2.00	2.00		

polyhedra are hosted, whereas the smaller one (B in Figure 3) hosts a single As2 site. Every successive layer is shifted (**b**-**a**)/3 along (0001); in this way, a smaller triangular cavity is superimposed on a larger one. Cu1 tetrahedron has bond-length ranging from 2.276(2) to 2.390(2) Å, whereas Cu2 is more regular, with bond-distances spanning through 2.370(2) and

2.390(2) Å. The Hg tetrahedron has a quite regular coordination, with bond-length between 2.470(2) and 2.502(2) Å; these distances are shorter than those observed by Kaplunnik et al. (1980) and Vasil'ev et al. (2010), indicating the possible substitution by a smaller cation for Hg. Table 6 reports the proposed site occupancies, the observed and the calculated site scattering. According to our results, Hg^{2+} is partially replaced by Cu^{+} and Ag^{+} at the Hg site; the electrostatic neutrality is restored through the substitution of Cu^{+} by higher-valency cations (Hg^{2+}, Zn^{2+}, Fe^{3+}) at the Cu2 site. This would explain the electron densities observed at these two sites. Nevertheless, the bond valence sums at these sites (Table 7) show significant valence excesses (up to +25% for Cu2 site), indicating too short Me–S distances. This could be the consequence of mean positions for the strongly mixed (Hg,Cu) and (Cu2,Hg) sites, as well as for their S ligands. Moreover, the minor Ag and Fe contents could not be located among the Hg and Cu sites, which explains why the structural formula of Table 2 is not perfectly charge-balanced.

The two independent As sites show bond distances ranging from 2.279(2) to 2.327(2) Å and are bonded, through corner-sharing, with CuS_4 and HgS_4 tetrahedra.

Following Krivovichev and Filatov (1999), Vasil'ev et al. (2010) also described the crystal structure of aktashite using an anion-centered approach. All S atoms are in fact arranged in cation tetrahedra, one vertex of which is As^{3+}, and others are Hg^{2+} and Cu^{+} cations. These S-centered tetrahedra form a three-dimensional framework characterized by the presence of an empty As_4 tetrahedron, with As–As distances ranging from 3.511 Å (As1–As1 distance) to 3.568 Å (As1–As2 distance). This small tetranuclear cluster $[As_4S_{12}]^{12-}$ (Figure 4) is probably the most interesting feature of the crystal structure of aktashite and has been accurately studied by Gabuda et al. (2009).

Crystal structure of laffittite

The crystal structure of laffittite is a three-dimensional framework formed by As-, Ag-, and Hg-centered polyhedra. Following the description given by Nakai & Appleman (1983) but assuming our cell setting (**a** and **c** have been permuted), the structure can be described as formed by (001) sheets of hexagonal rings of composition $AgHgAsS_3$, linked by corner

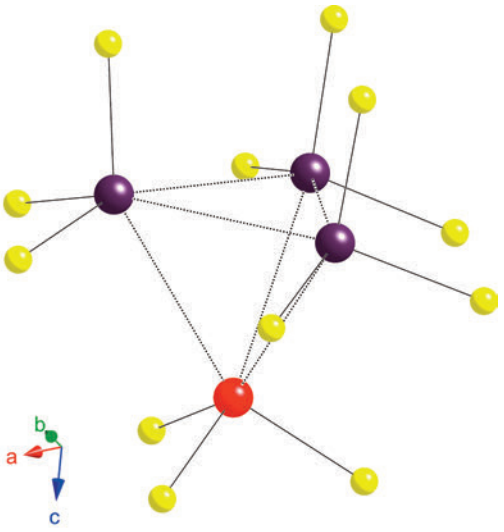

Figure 4. The $[As_4S_{12}]^{12-}$ cluster of aktashite. Symbols as in Figure 3.

sharing (Figure 5a). These sheets are linked, up and down, by Hg–S and Ag–S bonds. Using a polyhedral description, the (001) sheet is formed by Ag- and Hg-centered tetrahedra, with AsS_3 trigonal pyramids hosted in the triangular-like cavities of the layer. In laffittite, AsS_3 pyramids are isolated from each other (Figure 5b). In agreement with Nakai & Appleman (1983), there is another way to describe the crystal structure of this sulfosalt, that is considering the projection of the structure along **a*** (Figure 5c). In this way, a (100) sheet can be visualized, formed by two kinds of rings: a six-membered Ag_2HgS_3 ring and a ten-membered $AgHg_2As_2S_5$ ring. The interconnection of these rings gives rise to the (100) sheet. Along **a***, successive sheets are connected through As–S, Ag–S, and Hg–S bonds.

Table 5 gives selected bond distances for laffittite; the observed values are in agreement with those reported by Nakai & Appleman (1983) and Pervukhina et al. (2010a). Arsenic is at the vertex of a trigonal pyramid, with As–S bond-lengths ranging from 2.273 to 2.314 Å, slightly longer than those of laffittite from Getchell mine and in agreement with those of the specimen from Chauvai, Kyrgyzstan (Pervukhina et al., 2010a), owing to the Sb^{3+} to As^{3+} substitution. Ag atom has a (3+1) coordination, with three nearest S atoms at distances of 2.520(2), 2.529(2), and 2.616(2) Å, and one farther, at 2.910(2) Å. Hg atom shows a (2+2) distorted tetrahedral coordination, with two shorter bonds at 2.440(2) and 2.504(2) Å, and two longer ones, at 2.690(2) and 2.746(2) Å, with an average bond distance of 2.595 Å. The crystal structure agrees with the crystal chemical formula $AgHg(As_{0.92}Sb_{0.08})S_3$. Bond-valence balance results are reported in Table 7: contrary to those of aktashite, calculated values for laffittite are in good agreement with the theoretical ones, which is likely due to the lack of mixed cation sites.

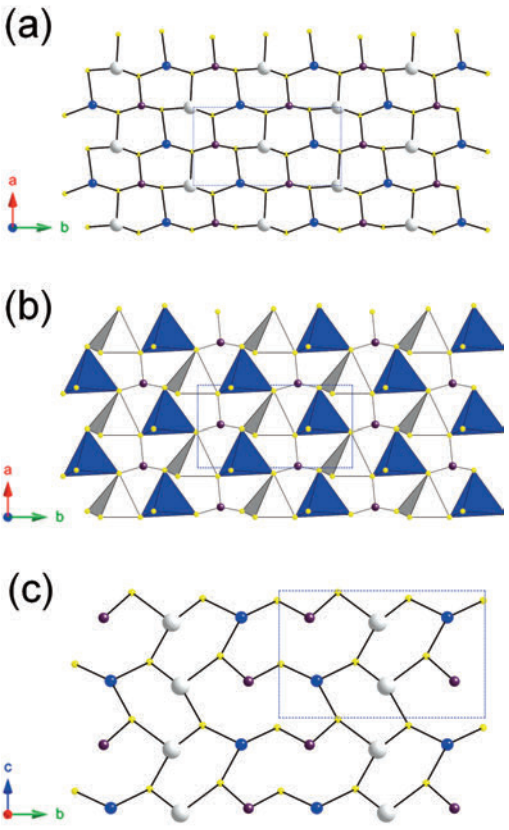

Figure 5. Crystal structure of laffittite. In (a) and (b) the crystal structure is seen down [001], whereas in (c) it is projected along [100]. Circles: grey = Ag site; blue = Hg site; violet = As site; and yellow = S sites.

Discussion

The refinements of the crystal structures of aktashite and laffittite allow us to discuss the coordination environment of Hg. Mercury shows two main kinds of coordination, linear and tetrahedral. Whereas the former is rather common, the latter is rarer and has been observed only in nine natural phases so far among sulfides and sulfosalts (Table 8). In addition, Hg assumes a tetrahedral coordination in Hg-bearing varieties of other phases, e.g., species belonging to the tetrahedrite group (e.g., Foit and Hughes, 2004; Pervukhina et al., 2010b) and in sphalerite (e.g., Grammatikopoulos et al., 2006; Radosavlievi ć et al., 2012).

Hg-centered tetrahedra can be regular, or distorted with two shorter and two longer bond distances. Aktashite and laffittite illustrate these two kinds of tetrahedral coordination environments (Figure 6). The former shows a regular tetrahedral coordination around Hg site (Figure 6a) and the average <Hg–S> bond distance observed in the specimen from Monte Arsiccio is similar to that observed by Chen and Szymański (1981) for the Hg site in galkhaite and by Biagioni et al. (2014) for the M1 site of arsiccioite. Actually, these sites have a mixed (Hg,Cu,Zn,Ag) occupancy, agreeing with the suggested substitution of Hg by Cu at the Hg site of aktashite. It is noteworthy that the <Hg–S> bond distance, in the studied specimens of aktashite (Table 8), is constantly lower than the ideal one, i.e. 2.576 Å for four-fold coordinated Hg, calculated using the bond-valence parameter R_{ij} given in Brese and O'Keeffe (1991). This could be in agreement with the substitution of Hg by smaller cations, like Cu and Zn. In particular, Zn is considered a substituent of Hg, giving the isotypic relationship between aktashite and nowackiite (Nowacki, 1982). As a matter of fact, chemical data of aktashite from Galkhaya (Kaplunnik et al., 1980), Aktash (Vasil'ev et al., 2010), and Monte Arsiccio (this work) do not report the occurrence of significant

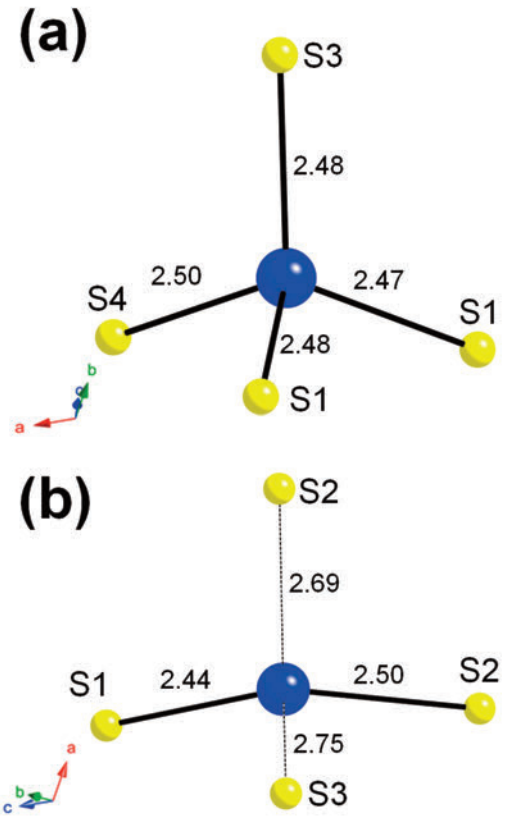

Figure 6. Hg-centered tetrahedra in aktashite (a) and laffittite (b). Solid and dashed lines indicates bond distances shorter and longer than 2.56 Å, respectively. Bond distances are expressed in Å.

Table 8. Sulfide and sulfosalt minerals with four-fold coordinated Hg. C.N. (coordination number) indicates the kind of coordination, as discussed in the text.

Mineral species	*Chemical formula*	*<Hg–S> (Å)*	*C.N.*	*Range (Å)*	*Ref.*
Aktashite - Galkhaya	$Cu_6Hg_3As_4S_{12}$	2.53	4	2.48 - 2.58	[1]
Aktashite - Aktash		2.503	4	2.491 - 2.528	[2]
Aktashite - Monte Arsiccio		2.481	4	2.470 - 2.502	[3]
Arsiccioite	$AgHg_2TlAs_2S_6$	2.473	4		[4]
		2.569	2+2	2.549 - 2.590	
Christite	$HgTlAsS_3$	2.560	2+2	2.460 - 2.661	[5]
Galkhaite	$(Cs,Tl)(Hg,Cu)_6(As,Sb)_4S_{12}$	2.496	4		[6]
Laffittite - Getchell	$AgHgAsS_3$	2.591	2+2	2.417 - 2.727	[7]
Laffittite - Chauvai		2.594	2+2	2.440 - 2.746	[8]
Laffittite - Monte Arsiccio		2.595	2+2	2.440 - 2.746	[3]
Metacinnabar	HgS	2.537	4		[9]
Metacinnabar - Bagnore		2.527	4		[10]
Routhierite - Jas Roux	$CuHg_2TlAs_2S_6$	2.512	2+2	2.481 - 2.543	[11]
Routhierite - Monte Arsiccio		2.563	2+2	2.502 - 2.621	[12]
Velikite	Cu_2HgSnS_4	2.569	4		[13]
Vrbaite	$Hg_3Tl_4As_8Sb_2S_{20}$	2.576	4	2.570 - 2.581	[14]

[1] Kaplunnik et al. (1980); [2] Vasil'ev et al. (2010); [3] this work; [4] Biagioni et al. (2014); [5] Brown and Dickson (1976); [6] Chen and Szymański (1981); [7] Nakai and Appleman (1983); [8] Pervukhina et al. (2010a); [9] Lehmann (1924);[10] unpublished data; [11] Bindi, 2008; [12] Biagioni et al., 2013a; [13] Kaplunnik et al. (1977); [14] Ohmasa and Nowacki (1971).

amounts of zinc in the studied specimens. Consequently, the smaller cation substituting Hg in tetrahedral coordination could be Cu. As indicated above, the occurrence of mixed Cu-Hg sites is known in minerals belonging to the tetrahedrite isotypic series and in the related mineral galkhaite (Moëlo et al., 2008); recently the same kind of site occupancy has been described in arsiccioite (Biagioni et al., 2014). The substitution of Hg^{2+} by Cu^{+} requires the introduction of Hg^{2+} replacing Cu^{+} at the Cu2 site, as discussed above. Whereas the <Cu–S> bond distance at the Cu1 site is 2.323 Å, in agreement with the <Cu–S> bond distance of the Cu site in chalcopyrite, that is 2.302 Å (Hall and Stewart, 1973), the average metal-sulfur distance

at the Cu2 site is larger, i.e. 2.380 Å. Foit and Hughes (2004) studied the structural variations in mercurian tetrahedrite. The average bond distance of the Cu-centered tetrahedron in the tetrahedrite structure increases from 2.338 to 2.371 Å for a tetrahedrite with a Hg content of 3 atom percent and 20 atom percent at the four-fold coordinated M1 site, respectively. These data are in agreement with a mixed (Cu,Hg) occupancy at the Cu2 site of aktashite.

Laffittite shows a distorted tetrahedral coordination around mercury atoms (Figure 6b). Typically, this kind of coordination can be described as a 2+2 coordination, with two shorter and two longer bonds. Arsiccioite, christite, laffittite, and routhierite are mineral species characterized by this kind of mercury coordination and the average <Hg–S> distances observed in these phases range between 2.560 and 2.595 Å. The only exception is represented by routhierite from Jas Roux, with Hg partially replaced by Zn and a consequent contraction of the tetrahedron size (Bindi, 2008). The constancy of the observed Hg–S bond distances in the studied specimens of laffittite from different occurrences suggests that no significant variation from the pure Hg occupancy at the Hg site occurs in this mineral.

This dissymmetry of Hg coordination in laffittite relatively to aktashite is closely related to the same kind of dissymmetry of the coordination of Ag in laffittite, relatively to that of Cu in aktashite (Table 5). It thus appears that Hg adapts the geometry of its coordination to that of monovalent transition metal, as Ag coordination is more easily distorted in sulfides and sulfosalts than Cu coordination, from dissymmetric tetrahedral up to binary linear. A good example of the close geometrical relationship between the linear coordination of Hg and Ag is the comparison of the crystal structures of rouxelite and neyite, respectively (Orlandi et al., 2005). According to Huheey et al. (1993), an increasing tendency to a linear coordination, according to the sequence Cu → Ag → Au ~ Hg, is related to the energy closeness between the $(n\text{-}1)d$ levels of the metal and its *ns* and *np* ones. In this way, the $(n\text{-}1)d_{z2}$ orbital reinforces the *sp* hybridization for a linear coordination.

Summary

In the Apuan Alps, mercury occurrences are rare and there are only two small Hg deposits, Levigliani and Ripa (Dini et al., 2001). Whereas an interesting mineral assemblage occurs at Levigliani (Dini et al., 1995), cinnabar is the only Hg mineral reported at Ripa. In addition to these occurrences, Hg-bearing phases were identified at other localities, in particular in the baryte-pyrite-iron oxides ore deposits. In fact, six different mercury minerals were identified at the Buca della Vena mine (cinnabar, coloradoite, marrucciite, metacinnabar, rouxelite, and tiemannite – Biagioni, 2009; Biagioni and Orlandi, 2009). The Monte Arsiccio mine exploited the same kind of ore deposits as Buca della Vena and displays a similar (but probably more complex) mineral assemblage, including extremely rare and unusual mercury sulfosalts, together with the complex Pb-Cu-Hg sulfosalt

rouxelite (third world occurrence – under study). The occurrence of aktashite, laffittite, routhierite, and the new mineral arsiccioite increases the numbers of sulfosalt species described from the hydrothermal veins of Apuan Alps and clearly exemplifies the exceptional Tl-Hg-As-Sb-(Ag,Cu)-Pb mineral assemblage of the Monte Arsiccio mine, which appears very similar to the Tl-rich mineralization of Jas Roux in the French Alps (Johan and Mantienne, 2000).

Acknowledgments

Electron microprobe analyses were performed with the help of J. Langlade (CNRS engineer, IFREMER Plouzané, France). The comments and corrections of two anonymous reviewers help us in improving the paper.

References

Biagioni C. (2009) - Minerali della Provincia di Lucca. Associazione Micro-mineralogica Italiana, Cremona, 352 p.

Biagioni C. and Orlandi P. (2009) - Tiemannite e metacinabro della miniera Buca della Vena (Alpi Apuane). *Atti della Società Toscana di Scienze Naturali*, *Memorie*, 114, 13-17.

Biagioni C., Orlandi P. and Pasero M. (2009) - Ankangite from the Monte Arsiccio mine (Apuan Alps, Tuscany, Italy): occurrence, crystal structure, and classification problems in cryptomelane group minerals. *Periodico di Mineralogia*, 78, 3-11.

Biagioni C., Bonaccorsi E., Moëlo Y. and Orlandi P. (2013a) - Mercury-arsenic sulfosalts from Apuan Alps (Tuscany, Italy). I. Routhierite, $(Cu_{0.8}Ag_{0.2})Hg_2Tl(As_{1.4}Sb_{0.6})_{\Sigma=2}S_6$, from Monte Arsiccio mine: occurrence and crystal structure. *European Journal of Mineralogy*, DOI: 10.1127/0935-1221/2013/0025-2320.

Biagioni C., D'Orazio M., Vezzoni S., Dini A. and Orlandi P. (2013b) - Mobilization of Tl-Hg-As-Sb-(Ag,Cu)-Pb sulfosalt melts during low-grade metamorphism in the Alpi Apuane. *Geology*, 41, 747-750.

Biagioni C., Bonaccorsi E., Moëlo Y., Orlandi P., Bindi L., D'Orazio M. and Vezzoni S. (2014) - Mercury-arsenic sulfosalts from the Apuan Alps (Tuscany, Italy). II. Arsiccioite, $AgHg_2TlAs_2S_6$, a new mineral from the Monte Arsiccio mine: occurrence, crystal structure and crystal chemistry of the routhierite isotypic series. *Mineralogical Magazine*, 78, 101-117.

Bindi L. (2008) - Routhierite, $Tl(Cu,Ag)(Hg,Zn)_2(As,Sb)_2S_6$. *Acta Crystallographica*, C64, i95-i96.

Brese N.E. and O'Keeffe M. (1991) - Bond-valence parameters for solids. *Acta Crystallographica*, B47, 192-197.

Brown K.L. and Dickson F.W. (1976) - The crystal structure of synthetic christite, $HgTlAsS_3$. *Zeitschrift für Kristallographie,* 144, 367-376.

Bruker AXS Inc. (2004) - APEX 2. *Bruker Advanced X-ray Solutions*, Madison, Wisconsin, USA.

Chen T.T. and Szymański J.T. (1981) - The structure and chemistry of galkhaite, a mercury sulfosalt containing Cs and Tl. *Canadian Mineralogist*, 19, 571-581.

Costagliola P., Benvenuti M., Tanelli G., Cortecci G. and Lattanzi P. (1990) - The barite-pyrite-iron oxides deposit of Monte Arsiccio (Apuane Alps). Geological setting, mineralogy, fluid inclusions, stable isotopes and genesis. *Bollettino della Società Geologica Italiana*, 109, 267-277.

Dini A., Benvenuti M., Lattanzi P. and Tanelli G. (1995) - Mineral assemblages in the Hg-Zn-Fe-S system at Levigliani, Tuscany, Italy. *European Journal of Mineralogy*, 7, 417-427.

Dini A., Benvenuti M., Costagliola P. and Lattanzi P. (2001) - Mercury deposits in metamorphic settings: the example of Levigliani and Ripa mines, Apuane Alps (Tuscany, Italy). *Ore Geology Reviews*, 18, 149-167.

Foit F.F.Jr. and Hughes J.M. (2004) - Structural variations in mercurian tetrahedrite. *American Mineralogist*, 89, 159-163.

Gabuda S., Kozlova S., Rizhikov M. and Borisov S. (2009) - Closed-shell interaction in the tetranuclear cluster As_4 in $Cu_6Hg_3As_4S_{12}$ crystal. *Journal of Molecular Structure: TEOCHEM*, 907, 62-65.

Grammatikopoulos T.A., Valeyev O. and Roth T. (2006)

- Compositional variation in Hg-bearing sphalerite from the polymetallic Eskay Creek deposit, British Columbia, Canada. *Chemie der Erde*, 66, 307-314.

Gruzdev V.S., Chernitsova N.M. and Shumkova N.G. (1972) - Aktashite - $Cu_6Hg_3As_5S_{12}$, new data. *Doklady Akademii Nauk SSSR*, 206, 694-697 (in Russian).

Hall S.R. and Stewart J.M. (1973) - The crystal structure refinement of chalcopyrite, $CuFeS_2$. *Acta Crystallographica*, B29, 579-585.

Huheey J.E., Keiter E.A. and Keiter R.L. (1993) - *Inorganic chemistry: Principles of structure and reactivity*. Harper Collins College Publischers.

Johan Z. and Mantienne J. (2000) - Thallium-rich mineralization at Jas Roux, Hautes-Alpes, France: a complex epithermal, sediment-hosted, ore-forming system. *Journal of the Czech Geological Society*, 45, 63-77.

Johan Z., Mantienne J. and Picot P. (1974) - La routhiérite, $TlHgAsS_3$, et la laffittite, $AgHgAsS_3$, deux nouvelles espèces minérales. *Bulletin de la Société Française de Minéralogie et de Cristallographie*, 97, 48-53.

Kaplunnik L.N., Pobedimskaya E.A. and Belov N.V. (1977) - Crystal structure of velikite, $Cu_{3.75}Hg_{1.75}Sn_2S_8$. *Kristallografiya*, 22, 99-100.

Kaplunnik L.N., Pobedimskaya E.A. and Belov N.V. (1980) - The crystal structure of aktashite $Cu_6Hg_3As_4S_{12}$. *Doklady Akademii Nauk SSSR*, 251, 96-98.

Krivovichev S.V. and Filatov S.K. (1999) - Structural principles for minerals and inorganic compounds containing anion-centered tetrahedra. *American Mineralogist*, 84, 1099-1106.

Lehmann W. (1924) - Roentgenographische untersuchungen an natuerlichem und synthetischem metacinnabarit (HgS). *Zeitschrift für Kristallographie*, 60, 379-413.

Martín-Izard A., Gumiel P., Arias M., Cepedal A., Fuertes-Fuente M. and Reguilón R. (2009) - Genesis and evolution of the structurally controlled vein mineralization (Sb-Hg) in the Escarlati deposit (León, Spain): Evidence from fault population analysis methods, fluid-inclusion research and stable isotope data. *Journal of Geochemical Exploration,* 100, 51-66.

Moëlo Y., Makovicky E., Mozgova N.N., Jambor J.L., Cook N., Pring. A., Paar W.H., Nickel E.H., Graeser S., Karup-Møller S., Balić-Žunić T., Mumme W.G., Vurro F., Topa D., Bindi L., Bente K. and Shimizu, M. (2008) - Sulfosalt systematics: a review. Report of the sulfosalt sub-committee of the IMA Commission on Ore Mineralogy. *European Journal of Mineralogy*, 20, 7-46.

Nakai I. and Appleman D.E. (1983) - Laffittite, $AgHgAsS_3$: crystal structure and second occurrence from the Getchell mine, Nevada. *American Mineralogist*, 68, 235-244.

Nowacki W. (1982) - Isotypy in aktashite $Cu_6Hg_3As_4S_{12}$ and nowackiite $Cu_6Zn_3As_4S_{12}$. *Soviet Physics - Crystallography*, 27, 26-27.

Ohmasa M. and Nowacki W. (1971) - The crystal structure of vrbaite, $Hg_3Tl_4As_8Sb_2S_{20}$. *Zeitschrift für Kristallographie*, 134, 360-380.

Orlandi P., Meerschaut A., Moëlo Y., Palvadeau P., and Léone P. (2005) - Lead-antimony sulfosalts from Tuscany (Italy). VIII. Rouxelite, $Cu_2HgPb_{22}Sb_{28}S_{64}(O,S)_2$, a new sulfosalt from Buca della Vena mine, Apuan Alps: Definition and crystal structure. *Canadian Mineralogist*, 43, 919-933.

Orlandi P., Biagioni C., Bonaccorsi E., Moëlo Y. and Paar W. (2012) - Lead-antimony sulfosalts from Tuscany (Italy). XII. Boscardinite, $TlPb_4(Sb_7As_2)_{\Sigma 9}S_{18}$, a new mineral species from Monte Arsiccio mine: occurrence and crystal structure. *Canadian Mineralogist*, 50, 235-251.

Orlandi P., Biagioni C., Moëlo Y., Bonaccorsi E., and Paar W. (2013) - Lead-antimony sulfosalts from Tuscany (Italy). XIII. Protochabournéite, ~ $Tl_2Pb(Sb_{9-8}As_{1-2})_{\Sigma 10}S_{17}$, from the Monte Arsiccio mine: occurrence, crystal structure, and relationship with chabournéite. *Canadian Mineralogist*, 51, 475-494.

Pervukhina N.V., Borisov S.V., Magarill S.A., Vasil'ev V.I. and Kuratieva N.V. (2010a) - Redetermination and crystallographic analysis of the structure of Sb-containing laffittite, $AgHg(As,Sb)S_3$ from Chauvai (Kyrgyzstan). *Journal of Structural Chemistry*, 51, 683-688.

Pervukhina N.V., Borisov S.V., Magarill S.A., Vasuliev V.I., Kuratieva N.V. and Kozlova S.G. (2010b) - Refinement of the crystal structure of As-schwatzite $Cu_6(Cu_{5.26}Hg_{0.75})(As_{2.83}Sb_{1.17})S_{13}$ (Aktash, Altai Mountaines). *Journal of Structural Chemistry*, 51, 898-903.

Powell W.G. and Pattison D.R. (1997) - An exsolution origin for low-temperature sulfides at the Hemlo gold deposit, Ontario, Canada. *Economic Geology*, 92, 569-577.

Radosavljević S.A., Stojanović J.N. and Pačevski A.M.

(2012) - Hg-bearing sphalerite from the Rujevac polymetallic ore deposit, Podrinje Metallogenic District, Serbia: compositional variations and zoning. *Chemie der Erde*, 72, 237-244.

Sheldrick G.M. (2008) - A short history of SHELX. *Acta Crystallographica*, A64, 112-122.

Spiridonov E.M., Krapiva L.Y., Stepanov V.I. and Chvileva T.N. (1981) - Antimony bearing aktashite from the Chauvay mercury deposit, Central Asia. *Doklady Akademii Nauk SSSR*, 261, 744-748 (in Russian).

Vasil'ev V.I. (1968) - New ore minerals of the mercury deposits of Gornyi Altai and thei parageneses. In: *Problems of the metallogeny of mercury*, Izdatelstvo "Nauka" Moskva, 111-129 (in Russian).

Vasil'ev V.I., Pervukhina N.V., Borisov S.V., Magarill S.A., Naumov D.Yu. and Kurat'eva N.V. (2010) - Aktashite $Cu_6Hg_3As_4S_{12}$ from the Aktash deposit, Altai, Russia: refinement and crystal chemical analysis of the structure. *Geology of Ore Deposits*, 52, 656-661.

Wilson A.J.C., Ed. (1992) - *International Tables for X-ray Crystallography*, Vol. C: Mathematical, physical and chemical tables. Kluwer Academic, Dordrecht, NL.

Submitted, September 2013 - Accepted, February 2014